Progress In Electromagnetics Research C, Vol. 108, 227–236, 2021

Efficient Isolation Modelling for Two-Port MIMO Antenna by Gaussian Process Regression

Kanhaiya Sharma[1, *] and Ganga Prasad Pandey[1, 2]

Abstract—This article presents a synthesis modelling of isolation in a diamond-shaped fractal electromagnetic band gag (DSFEBG) based two-port multiple input and multiple-output (MIMO) antenna using the Gaussian Process Regression (GPR). A compact two-port MIMO antenna with 0.140λ inter-element spacing is considered for isolation improvement. To predict mutual coupling in two-port MIMO antenna supervised learning-based regression technique of GPR, the model is trained with 50 samples and tested on 125 samples. The model performs result prediction in less than 1 second with RMSE less than 0.0001%. For a better understanding of the isolation between elements of the MIMO antenna, the automatic relevance determination property of GPR is presented. The proposed model does faster computation and is efficient in predicting isolation in DSFEBG based antennas for lower and high-frequency bands of 5G communication system.

1. INTRODUCTION

In the present COVID-19 scenario, there is a huge demand of bandwidth reliability due to the extreme use of video, audio, online meeting, and live data streaming in rural and urban areas. To improve radio frequency (RF) signal quality strength MIMO systems use multiple antennas. These antennae synchronously send the data to multiple users by sharing a single communication channel. At the transmission end, the RF signal is divided to feed into multiple antennas, then transmitted to the communication channel, and at the receiver end, multiple antennas are used to receive the signal efficiently. The receiver is designed in such a way that it can accommodate noise, lost signal, and the slight time difference between the receptions of signals. Mutual coupling (MC) effect on MIMO system or antenna arrays can be compensated either by the use of various stochastic optimization techniques or through various decoupling techniques. Stochastic optimization techniques are used to improve MIMO system parameters like channel capacity [1], energy and spectra efficiency [2], MIMO parameter optimization [3], MIMO antenna selection [4], designing and calibrating [5], and increase data throughput [6]. Researchers have investigated the effects of MC on the MIMO system in [7] and various decoupling techniques, and their optimum isolation value is in [8, 9]. A large body of evidence suggests that the defected ground structure and electromagnetic bandgap are a widely used technique to improve isolation value [10, 11]. Various fractal geometry is available [12] to design a multiband, electrically small, low side lobe array antenna and high directivity antenna. Designing and analysing a suitable decoupling structure for MIMO antenna is a time-consuming process and needs expertise. In the last two decades various simulation tools based on full-wave electromagnetic simulation have become popular and widely used by the microwave community. These tools provide the capabilities to design, simulate, and analyse different decoupling structures for improving isolation value in a MIMO system. There is a necessity

Received 3 December 2020, Accepted 7 January 2021, Scheduled 19 January 2021
* Corresponding author: Kanhaiya Sharma (sharmakanhaiya@gmail.com).
[1] Department of Computer Science and engineering, School of Technology, Pandit Deendayal Petroleum University, 382007, India.
[2] Department of Information and Communication Technology, School of Technology, Pandit Deendayal Petroleum University, 382007, India.

to have a method which can save time and accurately predict the isolation values of MIMO antenna based on learning. In available literature, machine learning technique has effectively addressed various problems of MIMO antenna like antenna selection [13, 14], optimum power allocation [15], antenna selection and power control [16], channel estimation [17], and fast beamforming [18]. Effectiveness of the GPR has been proved in existing works of literature to model, nonlinear problems of antenna [19]. GPR is highly effective in the modeling of various parameters of antenna-like radar cross-section [20], gain of antenna [21], modeling of microwave structures [22], and resonant frequency modeling [23]. In the present investigation, the authors investigate a regression-based highly accurate GPR model to predict isolation values in 2×2 MIMO for the lower frequency band of 5G. This article is summarized as follows. In Section 2, a brief discussion about GPR is explained. Section 3 describes the antenna design theory starting from a single antenna design followed by 2×2 MIMO antenna design along with isolation structure design. Section 4 describes model verification, and finally, in Section 5 conclusion is drawn out of the presented work.

2. GAUSSIAN PROCESS REGRESSION

This section describes the synthesis modelling of the stochastic GRP, to predict mutual coupling between two ports of a MIMO antenna. In ML, the GPR approach is used to solve supervised regression and classification based problems. The GPR modelling problem needs a training dataset of n input and output pairs $\{(p_i, q_i)|i = 1, 2, 3, \ldots, r\}$, where p_i is the input vector and collection of the dimension (d, dd, m, n) of decoupling structure, the height of material and dielectric constant, and q_i is the output vector of isolation values. The test dataset is independent from training dataset and contains r^* input and output pairs $\{(p_i^*, q_i^*)|i = 1, 2, 3, \ldots, r^*\}$. The GPR [19] describes that r training outputs are mapped to random variables $[f_1, f_2, f_3 \ldots f_r]^T = [f(p_1), f(p_2), f_(p3) \ldots f(p_r)]^T$, and the r^* test outputs by random variables $[f_1^*, f_2^*, f_3^* \ldots f_r^*]^T = [f(p_1)^*, f(p_2)^*, f_(p3)^* \ldots f(p_r)^*]^T$ with $f(\cdot)$ GP. A GP can be expressed as Gaussian distribution (GD) to function. For prediction, initially consider 0 mean Gaussian distribution over r training outputs and r^* test outputs [19]. This yields the prior distribution.

$$\begin{pmatrix} f \\ f^* \end{pmatrix} \sim B\left(0, \begin{bmatrix} S(P,P) & S(P,P^*) \\ S(P^*,P) & S(P^*,P^*) \end{bmatrix}\right) \tag{1}$$

where $S(a, b)$ denotes GD, here a is the mean vector and b a covariance matrix. P and P^* are training and test matrices, and $S(P, P^*)$ is an rxr^* submatrix of covariances calculated between training and test outputs. Next, compute posterior distribution for given q. The mean vector k and covariance matrix Σ are given by [19].

$$k = S(P^*, P)S(P, P)^{-1}q \tag{2}$$

$$\Sigma = S(P^*, P^*) - S(P^*, P)S(P, P)^{-1}S(P, P^*) \tag{3}$$

here q denotes isolation predictions. In the present article, five standard covariance functions are applied and named as exponential, squared exponential (SE), rational quadratic (RQ), matern 3/2, and matern 5/2 ones. The exponential kernel is defined as

$$k(p, p\prime) = \sigma_f^2 exp\left(-\sqrt{\sum_{l=1}^{d} \frac{(p_{il} - p_{jl})^2}{\sigma_l^2}}\right) \tag{4}$$

The exponential squared kernel is expressed as

$$k(a, a\prime) = \sigma_f^2 exp\left[\frac{-1}{2}\sum_{l=1}^{d} \frac{(p_{il} - p_{jl})^2}{\sigma_l^2}\right] \tag{5}$$

Rational quadratic kernel

$$k(p, p\prime) = \sigma_f^2 \left(1 + \frac{x^2}{2\alpha}\right)^{-\alpha} \tag{6}$$

Matern 3/2 kernel is expressed as follows

$$k(p, p\prime) = \sigma_f^2 \left(1 + \sqrt{3}x\right) \exp\left(-\sqrt{3x}\right) \tag{7}$$

Matern 5/2 kernel is expressed as

$$k(p, p\prime) = \sigma_f^2 \left(1 + \sqrt{5}x + \frac{5x^2}{3}\right) \exp\left(-\sqrt{5}x\right) \tag{8}$$

In Eqs. (6)–(8), the value of $x = \sqrt{\sum_{s=1}^{T} \frac{(p_{is} - p_{js})^2}{\sigma_s^2}}$, where p_{is} and p_{js} are the ith and jth components of input vectors p and $p\prime$ in the T-dimensional space, and σ_f and α are hyper parameters. In the present work, the following Gaussian likelihood is used to minimize the negative log marginal likelihood [19].

$$\log k(q|P) = \frac{-1}{2} q^T S^{-1} q - \frac{1}{2} \log |S| - \frac{r}{2} \log(2\pi) \tag{9}$$

where S is the $r \times r$ matrix; $S(P, P)$ is the the size of hyperparameter; σ_s is inversely proportional to influence on the regression, and this property is termed as automatic relevance property (ARP).

3. ANTENNA DESIGN THEORY

Initially, a single rectangular microstrip antenna designed at 2.4 GHz, on an FR-4 ($\epsilon_r = 4.4$) substrate with loss tangent $\tan\delta = 0.025$, is used and simulated with CST microwave studio 2019. The dimensions of the antenna are given as $L = 28.6\,\text{mm}$, $W = 38.37\,\text{mm}$, $h = 1.6\,\text{mm}$, $l_f = 10\,\text{mm}$, $w_f = 3.08\,\text{mm}$, feed length $(L_f) = 10\,\text{mm}$, and width $= (w_f) = 3.08\,\text{mm}$, and it is optimized for $50\,\Omega$ impedance. Subsequently, a two-port MIMO antenna is designed, with two identical elements placed 0.14λ apart from each other. The placement of elements is chosen in such a way that it can satisfy the diversity parameters of the MIMO system. The overall size of the 2×2 MIMO antenna is $39 \times 95.94\,\text{mm}^2$. In a microstrip antenna, surface waves produce losses that limit the overall performance of the antenna. The formation of band gap is calculated by the interplay between macroscopic and microscopic resonances of a periodic structure [24]. The most efficient way to suppress surface waves is to use EBG. EBG

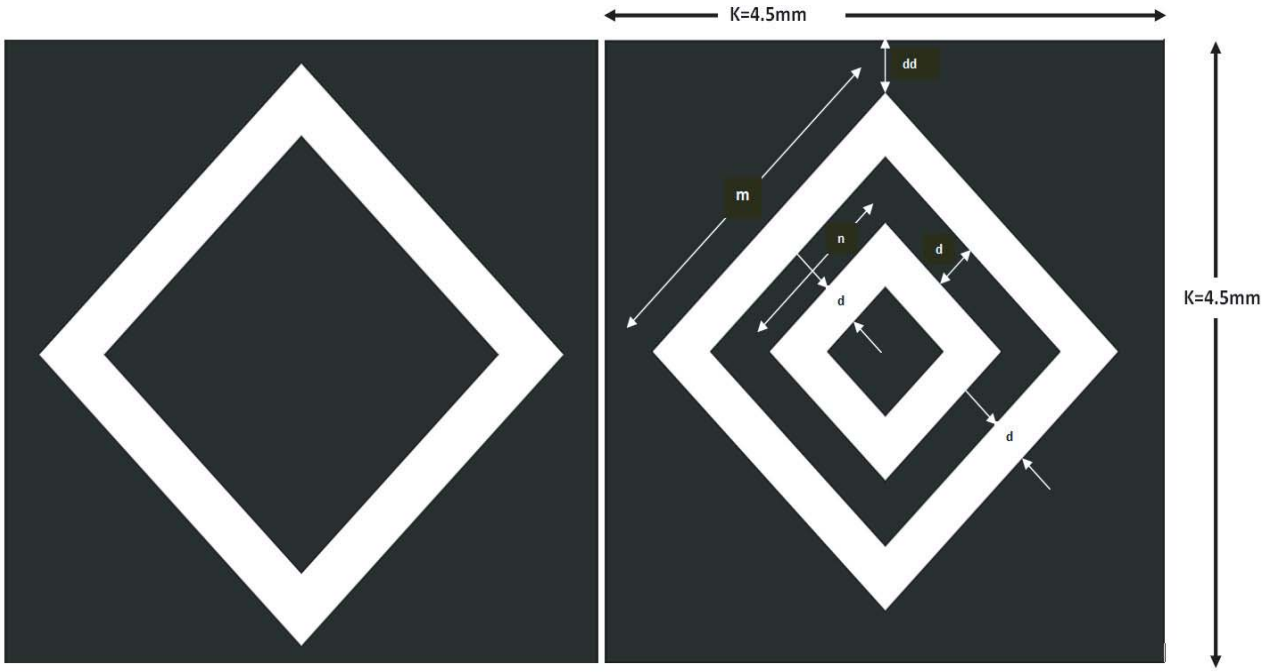

Figure 1. Schematic of DSFEBG iteration 1 and iteration 2.

Figure 2. Antenna geometry of 2×2 MIMO with DSFEBG structure.

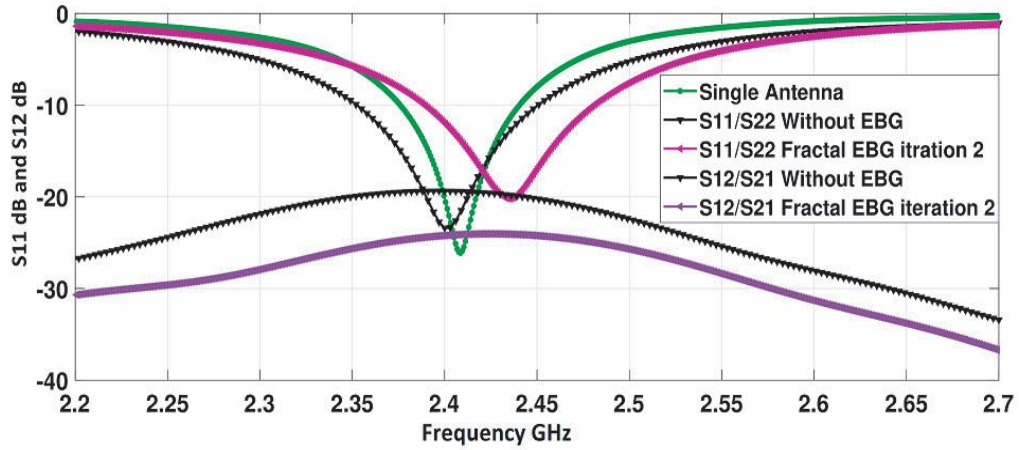

Figure 3. S parameter response for 2×2 MIMO antenna.

structures are periodic structures that are used to improve radiation characteristics, gain, and efficiency of the patch antenna. Due to high dielectric losses and surface waves, the isolation value of a two-port MIMO antenna is -19.35 dB. To improve isolation, 8 identical DSFEBGs are designed and placed at 4.5 mm apart from each other, with the same gap between two identical elements of MIMO. The dimensions of DSFEBGs are $d = 0.5$ mm, $dd = 0.38$ mm, $m = 2.82$ mm, $n = 1.41$ mm. The fractal iterations and geometry of the antenna are shown in Figs. 1 and 2. The detailed analysis of various fractal shapes EBGs is given by [25]. Return loss vs frequency plots for the single antenna and two-port MIMO antennas with and without an EBG structure are shown in Fig. 3. It is clear from evidence that the single antenna resonates at 2.4 GHz, and 2×2 MIMO antenna without any isolation structure resonates at slightly lower frequency due to mutual coupling. The antenna with a second iteration DSFEBG isolation structure resonates at 2.4462 GHz. It indicates the effect of the isolation structure on the proposed MIMO antenna. The isolation value of two-port MIMO antenna without an EBG structure is -19.35 dB and with EBG -24.67 dB, respectively. An improvement in an isolation value of 3.59 dB is reported after placing the fractal shaped EBG in between elements of MIMO.

4. MODEL VERIFICATION

DSFEBG decoupling structure is designed to improve isolation, and its geometry is shown in Fig. 1. The design vector is $p = [d\ dd\ m\ n\ kk\ h\ er]^T$, and its individual vector element ranges are given by $0.1 \leq d \leq 1.25$ mm, $0.1 \leq dd \leq 1.25$ mm, $0.00282 \leq m \leq 6.64674$ mm, $0.014241 \leq n \leq 1.779984$ mm, $0.045 \leq kk \leq 5.625$ mm, $1.1 \leq \epsilon_r \leq 13.5$, and $0.1 \leq h \leq 12.5$ mm, respectively. The other design parameters of two-port MIMO antenna like $L_g = 38.20$ mm, $W_g = 95.94$ mm, $L = 28.6$ mm, and $W = 38.37$ mm are kept fixed. Hundred and twenty-five data input vectors p are randomly sleeted from the design space using hypercube sampling (LHS) which are simulated in CST microwave studio 2019. Mutual coupling (S_{12}) value is determined from the maxima of the $|S_{12}|$ — vs frequency response. After data collection, the next five separate GPR models are trained according to the procedure described in Section 2. Five trained models, each utilizes a different covariance function and zero mean function from Eqs. (4)–(8) with the S_{12} values as training target t. The total training time to train all five models is approximately 17.79 seconds, and time is taken to train each model, give in Table 1. The configuration of the machine used to train and test models is as follows: Dell Inspiron 3521, X-64 based PC, Intel(R) Core (TM)i3-3217U CPU@ 1.8 GHz, 1801 MHz, two core(s), 4 logical processor(s) with installed physical memory (RAM) 6 GB on Microsoft Windows 10 education operating system. Model selection is made by selecting from the S_{12} models, the model that yields the lowest negative log marginal likelihood [19]. The model implementing the Matern 5/2 covariance function produces the lowest negative log marginal likelihood and gives the best result. From a total of 125 data samples, 75 samples are selected randomly to test model performance and predict S_{12}. Table 1 provides predictive accuracy in terms of root mean square errors (RMSEs) normalized to the S_{12} of the test target ranges, which are $12.56\,\text{dB} \leq S_{12} \leq 25\,\text{dB}$, and linear correlation coefficient R for prediction and target t. By observing Table 1, it is clear that highly accurate results have been achieved, with $\leq 0.0001\%$ error and correspondingly high correlation coefficient of 1. The scatter plot in Fig. 4 depicts the very close agreement between simulated and predicted S_{12}. After applying random search optimizer to Eqs. (4)–(8), RMSE and MAE can be further improved up to 4.5×10^{-5} and 3.2×10^{-5}, respectively with R^2 value 1. The model optimized in 181 seconds and 75 iterations is used to converge plot. Fig. 5 shows the minimum MSE plot, in which the red square indicates the iteration value corresponding to optimized hyperparameters, and the yellow point at iteration 5 shows hyperparameter at minimum MSE.

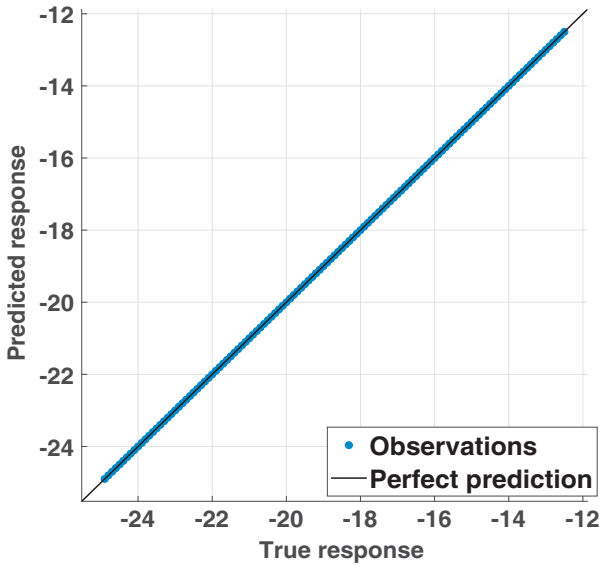

Figure 4. Scatter response against simulated and predicted S_{12}.

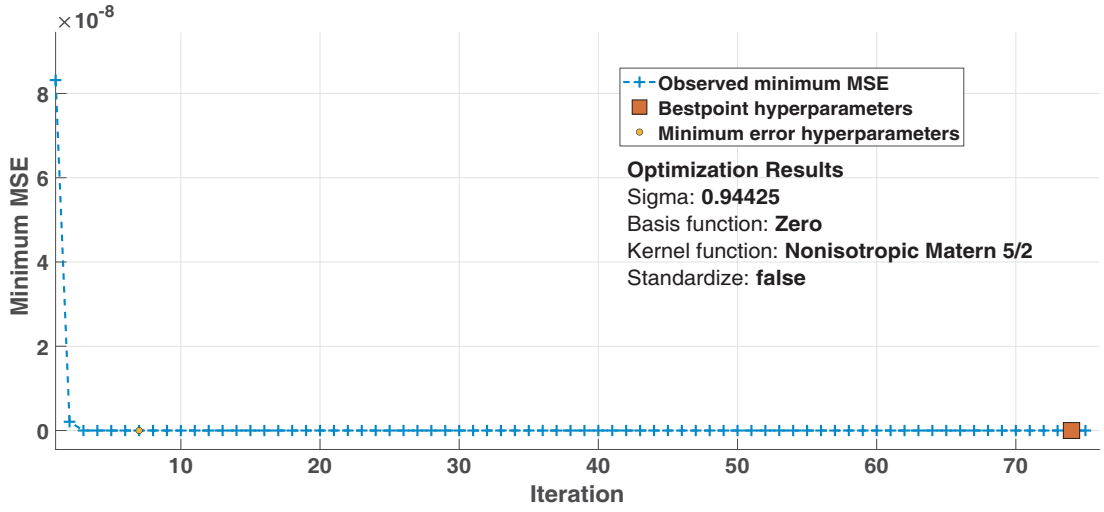

Figure 5. Optimized minimum MSE.

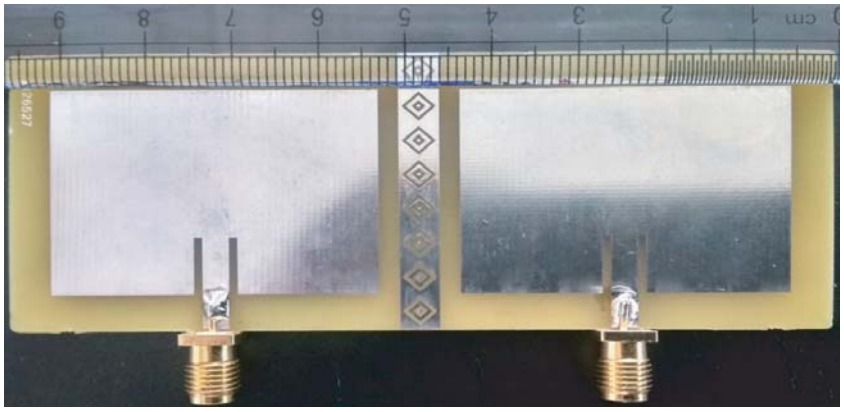

Figure 6. Fabricated tow port MIMO antenna.

Table 1. Prediction error on test dataset.

Training data samples = 50, and Testing data samples = 75					
	Covarience function				
Parameter	RQ	SE	Matern 3/2	Matern 5/2	Exponential
%RMSE	3.9×10^{-4}	3.9×10^{-4}	2.9×10^{-4}	1.3×10^{-4}	1.3×10^{-2}
R^2	1	1	1	1	1
%MAE	3.3×10^{-4}	3.3×10^{-4}	2.4×10^{-4}	1.1×10^{-4}	1.8×10^{-3}
Training time in sec	13.876	0.98151	0.9934	0.95562	0.98944

4.1. Fabrication and measurement

To verify the authenticity of the proposed GPR model, one sample was chosen randomly from test data and fabricated. Fig. 6 shows the fabricated antenna structure. S_{11} and S_{12} results of the fabricated antenna are measured using Anritsu Compact USB Vector Network Analyzer, model number MS46122B, which uses shockline VNA software for the graphical user interface (GUI). The simulated and measured results of the fabricated antenna are shown in Fig. 7. Simulated and measured values of S_{12} are -24.05 dB and -24.67 dB, respectively, which show close agreement. The radiation pattern without an

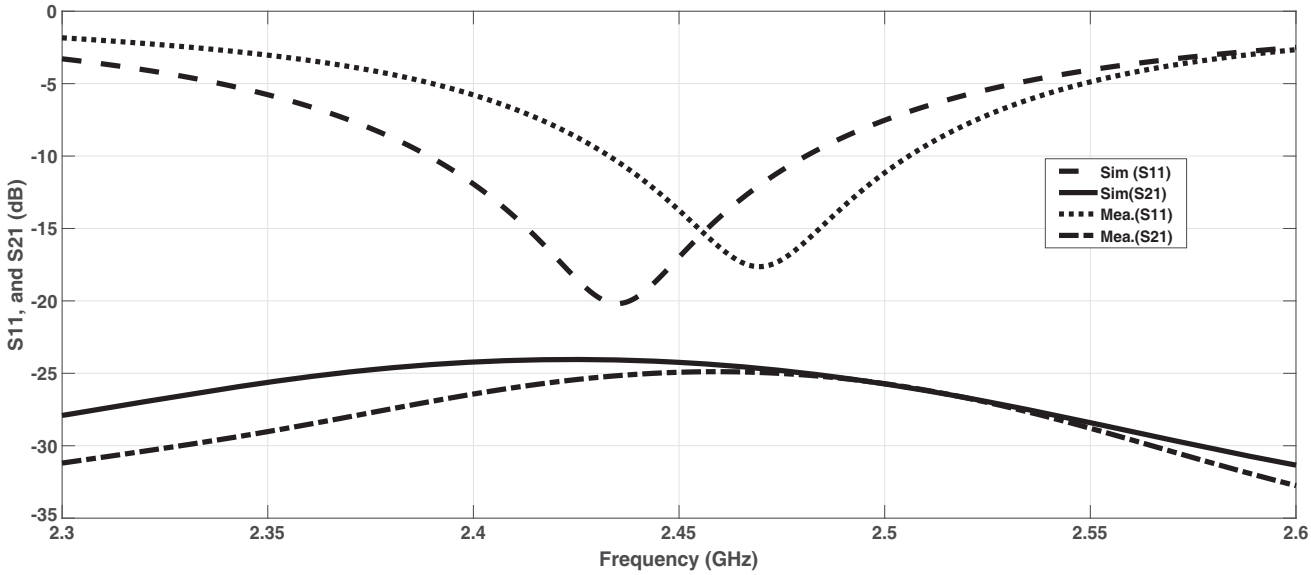

Figure 7. Simulated and measured S_{11}/S_{22} and S_{12}/S_{21} parameters.

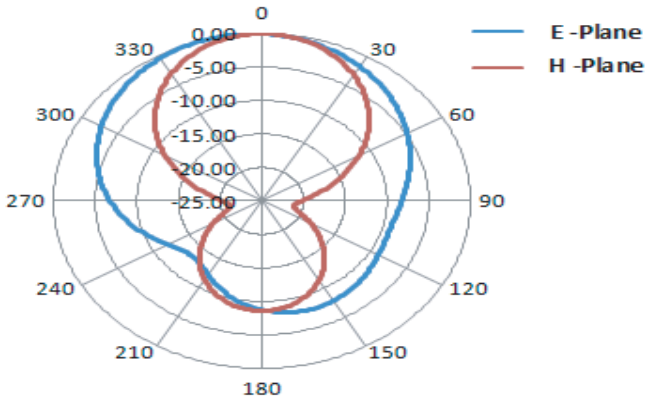

Figure 8. Radiation pattern without EBG.

EBG structure is shown in Fig. 8, and it is clear from the figure that the antenna radiates in broadside. The simulated and measured radiation patterns with a fractal-shaped EBG are shown in Fig. 9. It is clear from the evidence that there is a very close agreement between the simulated and measured patterns. The radiation efficiency and total efficiency of a two-port MIMO antenna without an EBG structure are 58.53%, 52.99%, and with fractal-shaped EBG 54.59%, 53.34%, respectively. Table 1 shows the performance of GPR model against RMSE, R^2 errors, and CPU time. It is also clear from the table that the proposed GPR technique quickly trains the model (< 1 second time). Table 2 shows the comparison of proposed 2×2 MIMO antennas with recently reported designs.

4.2. Automatic Relevance Determination

Minimizing negative log marginal likelihood provides optimal length scale parameter [23], information about input vector features. The lower the length scale parameter is related to a specific dimension of the input vector, the faster the changes occur in the actual function for that dimension. The values for length scale parameters are $d = 37.5\,\text{mm}$, $dd = 52.34\,\text{mm}$, $m = 73.65\,\text{mm}$, $n = 26.3\,\text{mm}$, $kk = 84\,\text{mm}$, $h = 14.9\,\text{mm}$ and $\epsilon_r = 10.4$. By looking at these parameters, it is clear that the most dominant variable ϵ_r is followed by h, n, and d for S_{12}.

Table 2. Comparison of proposed 2 × 2 MIMO antennas with recently reported designs.

References	MIMO	frequency	Isolation	ECC
[26]	2 × 2	2.4 GHz	15	0.1
[27]	2 × 2	2.4 GHz	19 dB	0.006
[28]	4 × 4	2.3–2.62 GHz & 3.46–10.3 GHz	18 dB	0.03
[29]	2 × 2	1.48–3.8 GHz	18 dB	0.01
[30]	2 × 2	2.35–3.05 GHz & 5.12–5.51 GHz	12 dB & 15 dB	0.001
[31]	2 × 2	2.38–2.47 GHz	20 dB	
[32]	2 × 2	2.31–2.51 GHz	17 dB	0.01
[33]	2 × 2	2.4–2.84 GHz	15	.003–.011
Proposed Antenna	2 × 2	2.43–2.50 GHz	−24.67 dB	0.0087

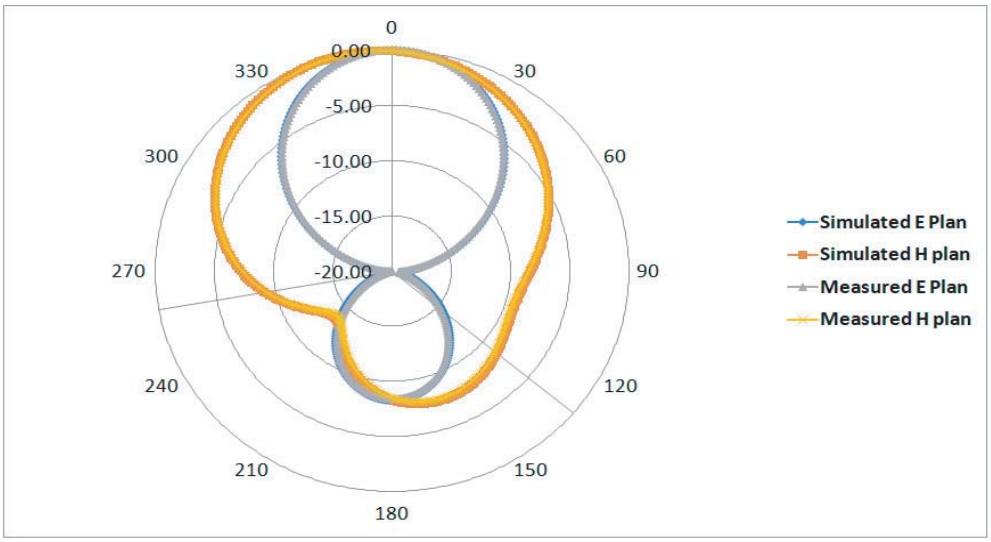

Figure 9. Simulated and measured radiation pattern.

5. CONCLUSION

In this work, machine learning based Gaussian Process Regression for the two-port MIMO antenna with DSFEBG has been presented and investigated experimentally. The RMSE and R^2 value of the synthesised model have been calculated and applied to validate the proposed model. For synthesised GPR model with input vectors $[d\ dd\ m\ n\ kk\ h\ er]^T$, the RMSE is 0.0001%; MAE is 1.82×10^{-8}; and R^2 is 1. Calculated error value shows that the proposed method is robust, fast in computation, and can be utilized to predict various parameters of a DSFEBG based antenna system for an advance wireless communication network.

REFERENCES

1. Recioui, A., "Application of a galaxy-based search algorithm to MIMO system capacity optimization," *Arabian Journal for Science and Engineering*, Vol. 41, 3407–3414, 2015.
2. Nimmagadda, S., "Optimal spectral and energy efficiency trade-off for massive MIMO technology: Analysis on modified lion and grey wolf optimization," *Soft Computing*, Vol. 14, 15523–15539, 2020.

3. Taieb, A., M. Soltani, and A. Chaari, "Parameter optimization of MIMO fuzzy optimal model predictive control by APSO," *Hindawi Complexity*, Vol. 2017, 11, 2017.
4. Ramya, P., R. S. Valarmathi, and C. Poongodi, "Antenna selection with Improved Group based Particle Swarm Optimization (IGPSO) and joint adaptive beam forming for wideband millimeter wave communication," *Journal of Ambient Intelligence and Humanized Computing*, 2020.
5. Hu, C., P. Lo, C. Ho, and D. Chang, "Automatic calibration using a modified genetic algorithm formillimeter-wave antenna modules in MIMO systems," *Hindawi International Journal of Antennas and Propagation*, Vol. 2020, 9, 2020.
6. Leal, I. A. C., M. S. Alencar, and W. T. A. Lopes, "Genetic algorithm optimization applied to the project of MIMO systems," *2017 25th International Conference on Software, Telecommunications and Computer Networks (SoftCOM)*, 1–5, 2017.
7. Chen, X., S. Zhang, and Q. Li, "A review of mutual coupling in MIMO systems," *IEEE Access*, Vol. 6, 24706–24719, 2018.
8. Malathi, A. C. J. and D. Thiripurasundari, "Review on isolation techniques in MIMO antenna systems," *Indian Journal of Science and Technology*, Vol. 9, No. 35, 2016.
9. Chouhan, S., D. K. Panda, M. Gupta, and S. Singhal, "Multiport MIMO antennas with mutual coupling reduction techniques for modern wireless transreceive operations: A review," *International Journal of RF and Microwave Computer-Aided Engineering*, Vol. 28, No. 2, e21189, 2018.
10. Wei, K., J. Li, L. Wang, Z. Xing, and R. Xu, "S-shaped periodic defected ground structures to reduce microstrip antenna array mutual coupling," *Electronics Letters*, Vol. 52, No. 15, 1288–1290, 2016.
11. Lee, J., S. Kim, and J. Jang, "Reduction of mutual coupling in planar multiple antenna by using 1-D EBG and SRR structures," *IEEE Transactions on Antennas and Propagation*, Vol. 63, No. 9, 4194–4198, Sep. 2015.
12. Anguera, J., C. Puente, C. Borja, and J. Soler, "Fractal shaped antennas: A review," American Cancer Society, 2005, Online, available: https://onlinelibrary.wiley.com/doi/abs/10.1002/0471654507.eme128.
13. Yang, P., J. Zhu, Y. Xiao, and Z. Chen, "Antenna selection for MIMO system based on pattern recognition," *Digital Communications and Networks*, Vol. 5, No. 1, 34–39, 2019.
14. An, W., P. Zhang, J. Xu, H. Luo, L. Huang, and S. Zhong, "A novel machine learning aided antenna selection scheme for MIMO internet of things," *Sensors (Basel, Switzerland)*, Vol. 20, No. 8, 2250, 2020.
15. Sanguinetti, L., A. Zappone, and M. Debbah, "Deep learning power allocation in massive MIMO," *2018 52nd Asilomar Conference on Signals, Systems, and Computers*, 1257–1261, 2018.
16. Vu, T. X., L. Lei, S. Chatzinotas, and B. Ottersten, "Machine learning based antenna selection and power allocation in multi-user MISO systems," *2019 International Symposium on Modeling and Optimization in Mobile, Ad Hoc, and Wireless Networks (WiOPT)*, 1–6, 2019.
17. Magoarou, L. L. and S. Paquelet, "Online unsupervised deep unfolding for massive MIMO channel estimation," *Signal Processing*, 2020.
18. Huang, H., W. Xia, J. Xiong, J. Yang, G. Zheng, and X. Zhu, "Unsupervised learning-based fast beamforming design for downlink MIMO," *IEEE Access*, Vol. 7, 7599–7605, 2019.
19. Rasmussen, C. E. and C. K. I. Williams, *Gaussian Processes for Machine Learning*, MIT Press, Cambridge, Massachusetts, 2006.
20. Jacobs, J. P. and W. P. du Plessis, "Efficient modeling of missile RCS magnitude responses by Gaussian processes," *IEEE Antennas and Wireless Propagation Letters*, Vol. 16, 3228–3231, 2017.
21. Jacobs, J. P., "Characterisation by Gaussian processes of finite substrate size effects on gain patterns of microstrip antennas," *IET Microwaves, Antennas and Propagation*, Vol. 10, No. 6, 1189–1195, Aug. 2016.
22. Jacobs, J. P. and S. Koziel, "Two-stage gaussian process modeling of microwave structures for design optimization," *Simulation-Driven Modeling and Optimization*, 161–184, S. Koziel, L. Leifsson, and X.-S. Yang, Eds., Springer International Publishing, Cham, 2016.

23. Jacobs, J. P., "Efficient resonant frequency modeling for dual-band microstrip antennas by Gaussian process regression," *IEEE Antennas and Wireless Propagation Letters*, Vol. 14, 337–341, 2015.
24. Alù, A., M. G. Silveirinha, A. Salandrino, and N. Engheta, "Epsilon-near-zero metamaterials and electromagnetic sources: Tailoring the radiation phase pattern," *Phys. Rev. B*, Vol. 75, 155410, Apr. 2007.
25. Krzysztofik, W. J., "Fractals in antennas and metamaterials applications," *Fractal Analysis*, F. Brambila (ed.), Ch. 3, IntechOpen, Rijeka, 2017.
26. Ryu, J. and H. Kim, "Compact MIMO antenna for application to smart glasses using T-shaped ground plane," *Microwave and Optical Technology Letters*, Vol. 60, No. 8, 2010–2013, 2018.
27. Su, S., C. Lee, and F. Chang, "Printed MIMO-antenna system using neutralization-line technique for wireless USB-dongle applications," *IEEE Transactions on Antennas and Propagation*, Vol. 60, No. 2, 456–463, Feb. 2012.
28. Kumar, S., R. Kumar, R. K. Vishwakarma, and K. Srivastava, "An improved compact MIMO antenna for wireless applications with band-notched characteristics," *AEU — International Journal of Electronics and Communications*, Vol. 90, 20–29, 2018.
29. Yang, Z., H. Yang, and H. Cui, "A compact MIMO antenna with inverted C-shaped ground branches for mobile terminals," *International Journal of Antennas and Propagation*, Vol. 2016, No. 3080563, 2016.
30. Dkiouak, A., A. Zakriti, M. E. Quahabi, A. Zugari, and M. Khalladi, "Design of a compact MIMO antenna for wireless applications," *Progress In Electromagnetics Research M*, Vol. 72, 115–124, 2018.
31. Anuvind, R., S. D. Joseph, and A. Kothari, "2 × 2 MIMO antenna at 2.4 GHz for WLAN applications," *2015 International Conference on Microwave, Optical and Communication Engineering (ICMOCE)*, 80–83, Dec. 2015.
32. Malviya, L., R. K. Panigrahi, and M. V. Kartikeyan, "2 × 2 MIMO antenna for ISM band application," *2016 11th International Conference on Industrial and Information System (ICIIS)*, 794–797, 2016.
33. Ayatollahi, M., Q. Rao, and D. Wang, "A compact, high isolation and wide bandwidth antenna array for long term evolution wireless devices," *IEEE Transactions on Antennas and Propagation*, Vol. 60, No. 10, 4960–4963, Oct. 2012.